

Transverse momentum dependence of semi-inclusive pion production

H. Mkrtchyan,¹ P.E. Bosted,^{2,3} G.S. Adams,⁴ A. Ahmidouch,⁵ T. Angelescu,⁶
J. Arrington,⁷ R. Asaturyan,¹ O.K. Baker,^{2,8} N. Benmouna,⁹ C. Bertoncini,¹⁰ H.P. Blok,¹¹
W.U. Boeglin,¹² H. Breuer,¹³ M.E. Christy,⁸ S.H. Connell,¹⁴ Y. Cui,¹⁵ M.M. Dalton,¹⁴
S. Danagoulian,⁵ D. Day,¹⁶ T. Dodario,¹⁵ J.A. Dunne,¹⁷ D. Dutta,¹⁸ N. El Khayari,¹⁵
R. Ent,² H.C. Fenker,² V.V. Frolov,¹⁹ L. Gan,²⁰ D. Gaskell,² K. Hafidi,⁷ W. Hinton,⁸
R.J. Holt,⁷ T. Horn,² G. M. Huber,²¹ E. Hungerford,¹⁵ X. Jiang,²² M. Jones,² K. Joo,²³
N. Kalantarians,¹⁵ J.J. Kelly,¹³ C.E. Keppel,^{2,8} V. Kubarovsky,² Y. Li,¹⁵ Y. Liang,²⁴
S. Malace,⁶ P. Markowitz,¹² E. McGrath,²⁵ P. McKee,¹⁶ D.G. Meekins,² B. Moziak,⁴
T. Navasardyan,¹ G. Niculescu,²⁵ I. Niculescu,²⁵ A.K. Opper,²⁴ T. Ostapenko,²⁶
P.E. Reimer,⁷ J. Reinhold,¹² J. Roche,² S.E. Rock,³ E. Schulte,⁷ E. Segbefia,⁸ C. Smith,¹⁶
G.R. Smith,² P. Stoler,⁴ V. Tadevosyan,¹ L. Tang,^{2,8} M. Ungaro,⁴ A. Uzzle,⁸
S. Vidakovic,²¹ A. Villano,⁴ W.F. Vulcan,² M. Wang,³ G. Warren,² F. Wesselmann,¹⁶
B. Wojtsekhowski,² S.A. Wood,² C. Xu,²¹ L. Yuan,⁸ X. Zheng,⁷ and H. Zhu¹⁶

¹*Yerevan Physics Institute, Yerevan, Armenia*

²*Thomas Jefferson National Accelerator Facility, Newport News, Virginia 23606*

³*University of Massachusetts Amherst, Amherst, Massachusetts 01003*

⁴*Rensselaer Polytechnic Institute, Troy, New York 12180*

⁵*North Carolina A & T State University, Greensboro, North Carolina 27411*

⁶*Bucharest University, Bucharest, Romania*

⁷*Physics Division, Argonne National Laboratory, Argonne, Illinois 60439*

⁸*Hampton University, Hampton, Virginia 23668*

⁹*The George Washington University, Washington, D.C. 20052*

¹⁰*Vassar College, Poughkeepsie, New York 12604*

¹¹*Vrije Universiteit, 1081 HV Amsterdam, The Netherlands*

¹²*Florida International University, University Park, Florida 33199*

¹³*University of Maryland, College Park, Maryland 20742*

¹⁴*University of the Witwatersrand, Johannesburg, South Africa*

¹⁵*University of Houston, Houston, TX 77204*

¹⁶*University of Virginia, Charlottesville, Virginia 22901*

¹⁷*Mississippi State University, Mississippi State, Mississippi 39762*

¹⁸*Triangle Universities Nuclear Laboratory and
Duke University, Durham, North Carolina 27708*

¹⁹*California Institute of Technology, Pasadena, California 91125*

²⁰*University of North Carolina Wilmington, Wilmington, North Carolina 28403*

²¹*University of Regina, Regina, Saskatchewan, Canada, S4S 0A2*

²²*Rutgers, The State University of New Jersey, Piscataway, New Jersey, 08855*

²³*University of Connecticut, Storrs, Connecticut 06269*

²⁴*Ohio University, Athens, Ohio 45071*

²⁵*James Madison University, Harrisonburg, Virginia 22807*

²⁶*Gettysburg College, Gettysburg, Pennsylvania 18103*

(Dated: October 24, 2018)

Abstract

Cross sections for semi-inclusive electroproduction of charged pions (π^\pm) from both proton and deuteron targets were measured for $0.2 < x < 0.5$, $2 < Q^2 < 4 \text{ GeV}^2$, $0.3 < z < 1$, and $P_t^2 < 0.2 \text{ GeV}^2$. For $P_t < 0.1 \text{ GeV}$, we find the azimuthal dependence to be small, as expected theoretically. For both π^+ and π^- , the P_t dependence from the deuteron is found to be slightly weaker than from the proton. In the context of a simple model, this implies that the initial transverse momenta width of d quarks is larger than for u quarks and, contrary to expectations, the transverse momentum width of the favored fragmentation function is larger than the unfavored one.

PACS numbers: 13.60.Le, 13.87.Fn

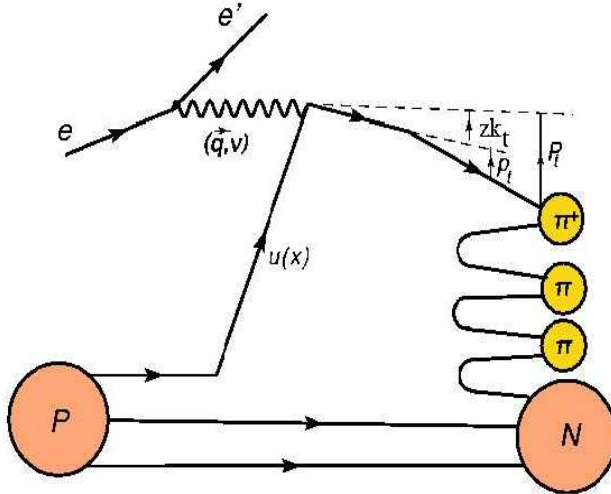


FIG. 1: Schematic diagram of semi-inclusive pion electroproduction within a factorized QCD parton model at lowest order in α_s . Final transverse momenta of the detected pion \vec{P}_t arises from convolving the struck quark transverse momenta \vec{k}_t with the transverse momentum generated during fragmentation process \vec{p}_t .

A central question in the understanding of nucleon structure is the orbital motion of partons. Much is known about the light-cone momentum fraction, x , and virtuality scale, Q^2 , dependence of the up and down quark parton distribution functions (PDFs) in the nucleon. In contrast, very little is presently known about the dependence of these functions on their transverse momentum k_t . Simply based on the size of the nucleon in which the quarks are confined, one would expect characteristic transverse momenta of order a few hundred MeV, with larger values at small Bjorken x where the sea quarks dominate, and smaller values at high x where all of the quark momentum is longitudinal in the limit $x = 1$. Increasingly precise studies of the nucleon spin sum rule [1, 2, 3, 4] strongly suggest that the net spin carried by quarks and gluons is relatively small, and therefore the net orbital angular momentum must be significant. This in turn implies significant transverse momentum of quarks. Questions that naturally arise include: what is the flavor and helicity dependence of the transverse motion of quarks and gluons, and can these be modeled theoretically and measured experimentally?

The process of semi-inclusive deep-inelastic lepton scattering (SIDIS), $lN \rightarrow lhX$ has been shown to factorize [5], in the high energy limit, into lepton-quark scattering followed

by quark hadronization. Ideally, one could directly measure the quark transverse momentum dependence of the quark distribution functions $q(x, k_t)$ by detecting all particles produced in the hadronization process. In the present experiment, we detect only a single hadronization product: a charged pion carrying an energy fraction z of the available energy. The probability of producing a pion with a transverse momentum P_t relative to the virtual photon (\vec{q}) direction is described by a convolution of the quark distribution functions and p_t -dependent fragmentation functions $D^+(z, p_t)$ and $D^-(z, p_t)$, where p_t is the transverse momentum of the pion relative to the quark direction, with the imposed condition [6] $\vec{P}_t = z\vec{k}_t + \vec{p}_t$ (see Fig. 1). The “favored” and “unfavored” functions $D^+(z, p_t)$ and $D^-(z, p_t)$ refer to the case where the produced pion contains of the same flavor as the struck quark or not. “Soft” non-perturbative processes are expected [6] to generate relatively small values of p_t with an approximately Gaussian distributions in p_t . Hard QCD processes are expected to generate large non-Gaussian tails for $p_t > 1$ GeV, and probably do not play a major role in the interpretation of the present experiment, for which the total transverse momentum $P_t < 0.45$ GeV. The assumption that the fragmentation functions do not depend on quark flavor (for example $D^+(z, p_t)$ applies equally well to $u \rightarrow \pi^+$ and $d \rightarrow \pi^-$) in principle allows the k_t widths of up and down quarks to be distinguished. In the present experiment, the use of both proton and deuteron targets (the latter with a higher d quark content than the former) and the detection of both π^+ and π^- permits a first study of this problem.

The experiment (E00-108) used the Short Orbit (SOS) and High Momentum (HMS) spectrometers in Hall C at Jefferson Lab to detect final state electrons and pions, respectively. An electron beam with energy of 5.5 GeV and currents ranging between 20 and 60 μA was provided by the CEBAF accelerator. Incident electrons were scattered from 4-cm-long liquid hydrogen or deuterium targets. The experiment consisted of three parts: i) at a fixed electron kinematics of $(x, Q^2) = (0.32, 2.30 \text{ GeV}^2)$, z was varied from 0.3 to 1, with nearly uniform coverage in the pion azimuthal angle, ϕ , around the virtual photon direction, but at a small average P_t of 0.05 GeV; ii) for $z = 0.55$, x was varied from 0.2 to 0.5 (with a corresponding variation in Q^2 , from 2 to 4 GeV^2), keeping the pion centered on the virtual photon direction (and again average P_t of 0.05 GeV); iii) for $(x, Q^2) = (0.32, 2.30 \text{ GeV}^2)$, z near 0.55, P_t was scanned from 0 to 0.4 GeV by increasing the HMS angle (with average ϕ near 180 degrees). The ϕ distribution as a function of P_t is shown for all three data sets combined in Fig. 2. The virtual photon-nucleon invariant mass W , was always larger than 2.1 GeV (typically

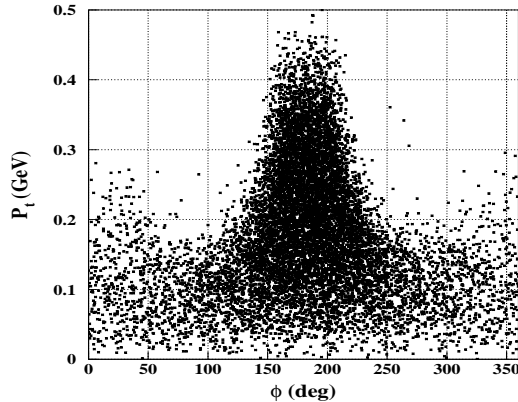


FIG. 2: P_t distribution of data from this experiment as a function of ϕ .

2.4 GeV), corresponding to the traditional deep inelastic region for inclusive scattering.

At lower virtual photon energy and/or mass scales, the factorization ansatz is expected to break down, due to the effects of final state interactions, resonant nucleon excitations, and higher twist contributions [7]. In particular, in the present experiment the residual invariant mass M_x of the undetected particles (see Fig. 1) ranges from about 1 to 2 GeV (inversely correlated with z), spanning the mass region traditionally associated with significant baryon resonance excitation. The extent to which this situation leads to a break-down of factorization was studied in our previous paper [8]. It was found that good agreement with expectations based on higher energy data was achieved for $z < 0.7$, approximately corresponding to $M_x > 1.5$ GeV. The ratio of total up to down quark distributions $u(x)/d(x)$ extracted from ratios of cross sections, as well as the ratio of valence-only up to down ratios $u_v(x)/d_v(x)$, were also found to be reasonably compatible with higher energy extractions, provided $z < 0.7$. This issue will be addressed further for the P_t -scan data below. Finally, the ratio of unfavored to favored fragmentation functions $D^-(z)/D^+(z)$ (from the π^-/π^+ ratios on the deuteron) was found to be consistent with extractions from other experiments. All of these studies were done with the z -scan and x -scan data, for which the average P_t was small (< 0.1 GeV), and the average value of $\cos(\phi)$ was close to zero.

In this paper, we focus on the P_t dependence, with the goal of searching for a possible flavor dependence to the quark distribution functions and/or fragmentation functions. Since the average value of $\cos(\phi)$ in the present experiment is correlated with P_t (approaching -1

for the largest P_t value of 0.45 GeV, see Fig. 2), we first study the limited data available from this experiment on the ϕ dependence, which must be an even function since neither the beam nor the target were polarized. We parameterize [9] the data for each target and pion flavor according to:

$$\frac{d\sigma_{ee'\pi x}}{d\sigma_{ee'x}} = \frac{dN}{dz} b \exp(-bP_t^2) \frac{1 + A \cos \phi + B \cos(2\phi)}{2\pi} \quad (1)$$

where the parameters $A(x, Q^2, z, P_t)$ and $B(x, Q^2, z, P_t)$ are a measure of the relative importance of the interference terms σ_{LT} and σ_{TT} , respectively [10]. The assumed Gaussian P_t^2 dependence (with slopes b for each case) is an effective parameterization that seems to describe the data adequately for use in making radiative and bin-centering corrections. We use this model for studying the ϕ dependence, then return to a more detailed study of the P_t dependence in the context of a simple model that incorporates a different P_t dependence for each struck quark and produced hadron flavor.

For each kinematic point in the x and z scans (average $P_t = 0.05$ GeV, maximum P_t 0.2 GeV), we extracted A and B and found no statistically significant difference between the results for π^+ or π^- , or proton or deuteron targets. We therefore combined all four cases together, and present the results in Fig. 3. Systematic errors (not shown in the figure) are approximately 0.03 on both A and B and are highly correlated from point to point. Taking the systematic errors into account, the values of A and B are close to zero, for all values of x studied, and for values of $z < 0.7$, where our previous studies showed a good consistency with factorization. The small values of A and B are also consistent with the expectations based on kinematic shifts due to parton motion as described by Cahn [11] (shown as the solid curves on the figures) and Levelt-Mulders [12]. These effects are proportional to P_t for A , and P_t^2 for B respectively [11, 12, 13, 14], so are suppressed at low P_t . More specifically, using the assumption that the average quark and fragmentation widths are equal, the Cahn [11] asymmetries are given by

$$A = -\gamma(2 \langle P_t \rangle / Q)(2 - y)\sqrt{1 - y}/[1 + (1 - y)^2], \quad (2)$$

$$B = -\gamma^2(2 \langle P_t^2 \rangle / Q^2)(1 - y)/[1 + (1 - y)^2], \quad (3)$$

where $\gamma = z^2/(1 + z^2)$, $y = \nu/E$, ν is the virtual photon energy, and E is the beam energy, yielding $A = -0.01$ and $B = -0.0002$ for $z = 0.55$. The more recent treatment of Ref. [6] also gives results for A and B which are very close to zero (especially for B). Other possible

higher twist contributions will also be proportional to powers of $P_t/\sqrt{(Q^2)}$ [15, 16], and therefore suppressed at our lower average values of P_t and P_t^2 . Specifically, the twist-2 Boer-Mulders [17] contribution to B is essentially zero in the models of Ref. [17, 18].

In contrast, the longitudinal-transverse and transverse-transverse coefficients A and B are much larger in exclusive pion production ($M_x = M$, where M is the nucleon mass) than those predicted for SIDIS. This is evidenced by our extracted average values for exclusive π^\pm electroproduction on deuteron and for π^+ on proton, shown as the open symbols near $z = 0.98$ in Fig. 3. This underlines the importance of accounting for the radiative tail from exclusive production, which in our analysis was done using the computer code EXCLURAD [19] together with a reasonable model of exclusive pion electroproduction. The corrections were checked with the Hall C simulation package SIMC, which treats radiative corrections in the energy and angle peaking approximation [20].

We now turn to the study of the P_t scan data. We used the cross section model from our previous paper [8] to describe the Q^2 dependence of the data (needed because P_t and Q^2 are somewhat correlated), and extracted cross sections at fixed Q^2 averaged over ϕ . The corrections for Q^2 dependence did not distinguish between targets or pion flavor. Relatively small corrections (typically a few percent) for radiative effects (including the tails from exclusive pion production) and diffractive ρ production were made [8] for each case individually. The systematic error on these corrections is estimated to be approximately 2%. The normalization errors due to target thickness, computer and electronic dead time, beam charge measurement, beam energy, and spectrometer kinematics combine to approximately 2% overall, and 1% from case to case. The overall error due to spectrometer acceptance is estimated to be 3%, but $< 1\%$ from case to case because targets were exchanged frequently, as was the spectrometer polarity. The extracted cross sections are shown in Fig. 4 and listed in Table I. The acceptance-averaged values of $\cos(\phi)$ range from -0.3 at low P_t to nearly -1 at higher P_t , while the average values of $\cos(2\phi)$ approaches 1 at high P_t (See Fig. 2 and Table I).

Examination of Fig. 4 shows that the P_t -dependence for π^+ and π^- are very similar to each other for each target, but that the slopes for the deuteron target are somewhat smaller than those for the proton. For a more quantitative understanding of the possible implications, we study the data in the context of a simple model in which the P_t dependence is described in terms of two Gaussian distributions for each case. Following Ref. [6], we assume that the

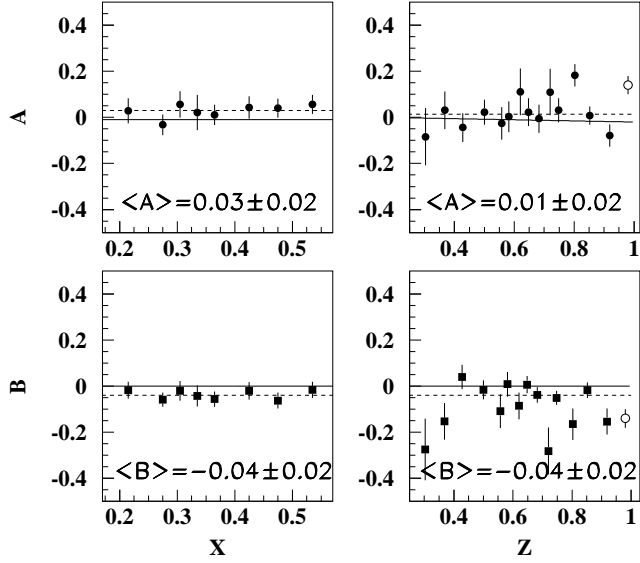


FIG. 3: The parameters A and B [the relative coefficients of the $\cos\phi$ (σ_{LT}) and $\cos 2\phi$ (σ_{TT}) terms] averaged over π^+ and π^- detected from proton and deuteron targets, as a function of x at $\langle z \rangle = 0.55$ (left), and as a function of z at $\langle x \rangle = 0.32$ (right). The average value of transverse momentum ($\langle |P_t| \rangle$) is ~ 0.05 GeV. The dashed lines indicate the weighted averages for $z < 0.7$, which are also enumerated in each panel. Errors indicated include only statistical contributions. Systematic errors are highly correlated from point to point, and are estimated at 0.03 on both A and B . The open symbols are from exclusive pion production (see text). The solid lines are theoretical predictions [11].

widths of quark and fragmentation functions are Gaussian in k_t and p_t , respectively, and that the convolution of these distributions combines quadratically. The main difference from Ref. [6] is that we allow separate widths for up and down quarks, and separate widths for favored and unfavored fragmentation functions. The widths of the up and down distributions are given by μ_u and μ_d , respectively, and the favored (unfavored) fragmentation widths are given by μ_+ (μ_-). Following Cahn [11] and more recent studies [6], we assume that only the fraction z of the quark transverse momentum contributes to the pion transverse momentum

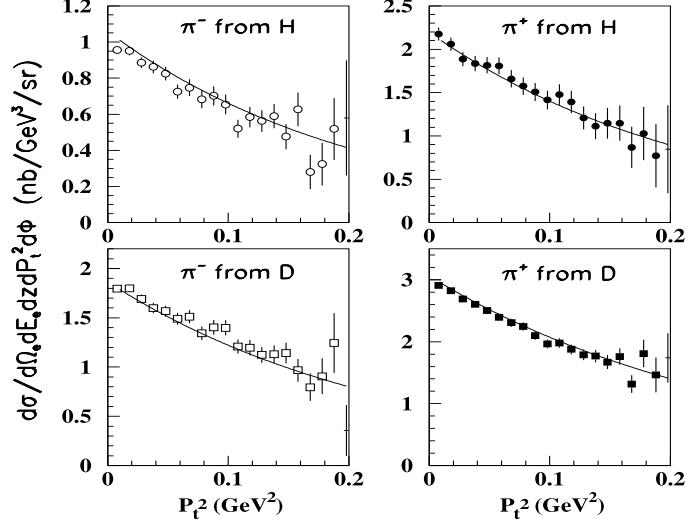


FIG. 4: The P_t^2 dependence of differential cross-sections per nucleus for π^\pm production on hydrogen (H) and deuterium (D) targets at $\langle z \rangle = 0.55$ and $\langle x \rangle = 0.32$. The solid lines show the result of the seven-parameter fit described in the text. The error bars are statistical only. Systematic errors are typically 4% (relative, see text for details). The average value of $\cos(\phi)$ varies with P_t^2 (see Table 1).

(see Fig. 1). We assume further that sea quarks are negligible (typical global fits show less than 10% contributions at $x = 0.3$). To make the problem tractable, we take only the leading order terms in (k_t/Q) , which was shown to be a reasonable approximation for small to moderate P_t in Ref. [6]. The simple model can then be written as:

$$\begin{aligned}
\sigma_p^{\pi^+} &= C[4c_1(P_t)e^{-b_u^+ P_t^2} + (d/u)(D^-/D^+)c_2(P_t)e^{-b_d^- P_t^2}] \\
\sigma_p^{\pi^-} &= C[4(D^-/D^+)c_3(P_t)e^{-b_u^- P_t^2} + (d/u)c_4(P_t)e^{-b_d^+ P_t^2}] \\
\sigma_n^{\pi^+} &= C[4(d/u)c_4(P_t)e^{-b_d^+ P_t^2} + (D^-/D^+)c_3(P_t)e^{-b_u^- P_t^2}] \\
\sigma_n^{\pi^-} &= C[4(d/u)(D^-/D^+)c_2(P_t)e^{-b_d^- P_t^2} + c_1(P_t)e^{-b_u^+ P_t^2}]
\end{aligned} \tag{4}$$

where C is an arbitrary normalization factor, and the inverse of the total widths for each

combination of quark flavor and fragmentation function are given by

$$\begin{aligned} b_u^\pm &= (z^2 \mu_u^2 + \mu_\pm^2)^{-1} \\ b_d^\pm &= (z^2 \mu_d^2 + \mu_\pm^2)^{-1} \end{aligned} \tag{5}$$

and we assume $\sigma_d = (\sigma_p + \sigma_n)/2$. The Cahn effect [6, 11] is taken into account through the terms:

$$\begin{aligned} c_1(P_t) &= 1. + c_0(P_t, \langle \cos(\phi) \rangle) \mu_u^2 b_u^+ \\ c_2(P_t) &= 1. + c_0(P_t, \langle \cos(\phi) \rangle) \mu_d^2 b_d^- \\ c_3(P_t) &= 1. + c_0(P_t, \langle \cos(\phi) \rangle) \mu_u^2 b_u^- \\ c_4(P_t) &= 1. + c_0(P_t, \langle \cos(\phi) \rangle) \mu_d^2 b_d^+ \\ c_0(P_t, \langle \cos(\phi) \rangle) &= \frac{4z(2-y)\sqrt{1-y}}{\sqrt{Q^2[1+(1-y)^2]}} \sqrt{P_t^2} \langle \cos(\phi) \rangle. \end{aligned} \tag{6}$$

We fit for the four widths (μ_u , μ_d , μ_+ , and μ_-), C , and the ratios D^-/D^+ and d/u , where the fragmentation ratio is understood to represent the data-averaged value at $z = 0.55$, and the quark distribution ratio is understood to represent the average value at $x = 0.3$. The fit describes the data reasonably well ($\chi^2 = 78$ for 73 degrees of freedom), and finds the somewhat low ratio $d/u = 0.30 \pm 0.03$ (the LO GRV98 fit [21] has about 0.40 for valence quarks), and the more reasonable ratio $D^-/D^+ = 0.42 \pm 0.01$ (a fit to HERMES results [22], $D^-/D^+ = 1/(1+z)^2$, predicts 0.42 at $z = 0.55$). Both d/u and D^-/D^+ are largely uncorrelated with other fit parameters. Since the data are at fixed z , the main contributions that distinguishes large fragmentation widths from large quark widths are the ϕ -dependence Cahn-effect c_i terms. While there is a significant inverse correlation between the two most important quark and fragmentation widths, (μ_u and μ_+ , respectively), the fit finds a clear preference for μ_u to be smaller than μ_+ as shown in Fig. 5a. On the other hand, the fit finds μ_d and μ_- to be of the same magnitude and not strongly correlated, as shown in Fig. 5b.

The fit tends to favor a larger k_t width for d quarks ($\mu_d^2 = 0.22 \pm 0.13 \text{ GeV}^2$) than for u quarks ($\mu_u^2 = -0.01 \pm 0.04 \text{ GeV}^2$), as illustrated in Fig. 5c, although the error on the d quark width is relatively large. The tendency is consistent with a di-quark model [23] in which the d quarks are only found in an axial di-quark, while the u quarks are predominantly found in a scalar di-quark. If the axial and scalar di-quarks have different masses, for example 0.9 and 0.6 GeV, then the d quark distribution falls off more slowly with k_t than the u quark distribution. In this model, the distributions show considerable deviation from an

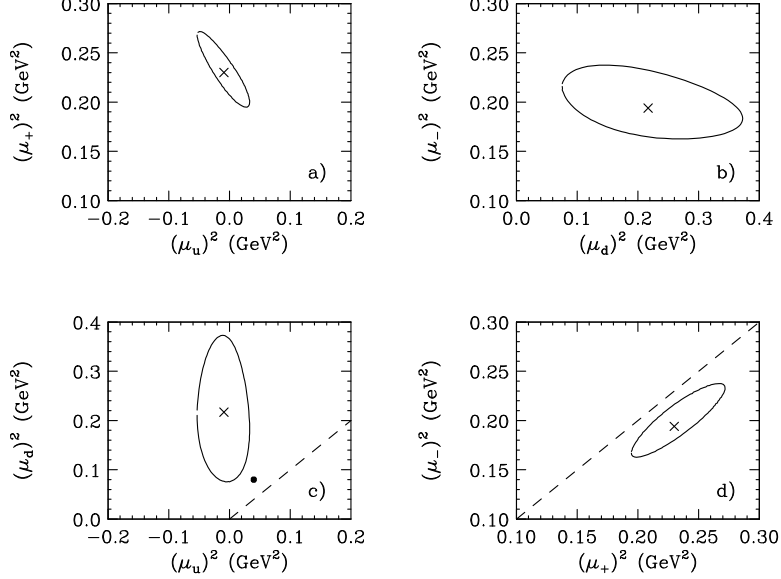


FIG. 5: Fit parameters (crosses) and two-standard-deviation contours from the seven-parameter fit to the data shown in Fig. 3: a) u quark width squared μ_u^2 versus favored fragmentation width squared μ_+^2 ; b) μ_d^2 versus μ_-^2 ; c) μ_u^2 versus μ_d^2 ; d) μ_-^2 vs μ_+^2 . The large dot near the bottom of panel c is from a di-quark model [23]. The dashed line in panels c and d indicate $\mu_u^2 = \mu_d^2$ and $\mu_-^2 = \mu_+^2$, respectively.

exponential falloff, but if we take the slope at the origin, the corresponding widths are $\mu_u^2 = 0.04$ and $\mu_d^2 = 0.08$ GeV², as illustrated by the solid dot in Fig. 5c. Fixing the quark widths to these values still gives a reasonable fit to our data ($\chi^2 = 81$ for 75 degrees of freedom). The magnitude of both widths is moderately sensitive to the choice of the model parameter λ_0 (we used 0.6 GeV), although the difference in widths is largely driven by the difference in axial and scalar di-quark masses (for example, increasing the axial di-quark mass to 1.4 GeV increases μ_d^2 to 0.25 GeV², which is the central value of our fit). Using the fit parameters, we find the magnitude of the $\cos(\phi)$ term A (Eq. 2) at $P_t = 0.4$ GeV to be about -0.05 for all cases except π^+ production from hydrogen, where it is 0.01. These results are similar in sign and magnitude to those found in the HERMES experiment [24].

We find that the fragmentation widths μ_+ and μ_- are correlated, as illustrated in Fig. 5d, although the allowed range is not large, and the central values ($\mu_+^2 = 0.23 \pm 0.04$ GeV² and $\mu_-^2 = 0.19 \pm 0.04$ GeV²) are in reasonable agreement with both each other and also the flavor-averaged value of 0.20 GeV² found in Ref. [6]. While there is a slight tendency for the

avored width to be larger than the unfavored one, a reasonable fit can be obtained setting the widths equal to each other ($\chi^2 = 81$ for 74 d.f., $\mu_+^2 = \mu_-^2 = 0.22 \pm 0.04 \text{ GeV}^2$).

To estimate the effect of experimental systematic errors on our fit results, we repeated the fits with: no diffractive ρ subtraction; no exclusive radiative tail subtraction; relative target thickness changed by 1%; and difference in π^+ and π^- absorption changed by 1%. In all cases, the quark and fragmentation width results remained well within the error ellipses shown in Fig. 5. The only parameter that changed significantly is the d/u ratio, which goes up to 0.33 with no exclusive tail subtraction. We found no significant change to the fit parameters upon adding to μ_u^2 and μ_d^2 an average nucleon transverse momentum squared of 0.001 GeV^2 (evaluated using the Paris wave function [25]) for the deuteron model.

In summary, we have measured semi-inclusive electroproduction of charged pions (π^\pm) from both proton and deuteron targets, using 5.5 GeV energy electrons at Jefferson Lab. We find the azimuthal dependence to be small, compared to exclusive pion electroproduction, and consistent with theoretical expectations [6, 11]. In the context of a simple model with only valence quarks and only two fragmentation functions, we find the k_t width of d quarks to be larger than for u quarks, for which the width is consistent with zero within the statistical error. We find that the favored fragmentation p_t width to be (unexpectedly) somewhat larger than the unfavored width, although both are larger than the u quark width.

All of the above fit results can only be considered as suggestive at best, due to the limited kinematic range covered, the somewhat low u/d ratio that we find, and the very simple model assumptions described above. Many of these limitations could be removed with future experiments covering a wide range of Q^2 (to resolve additional higher twist contributions), full coverage in ϕ , a larger range of P_t , a wide range in z (to distinguish quark width terms, which is weighted by powers of z , from fragmentation widths, which likely vary slowly with z), and including the π^0 final state for an additional consistency check (particularly on the assumption that only two fragmentation functions are needed for charged pions from valence quarks). Some of these goals should be attainable with existing and upcoming data from Jefferson Lab, especially after the planned energy upgrade. These data should provide potential information on how hadron transverse momentum in SIDIS is split between fragmentation and intrinsic quark contributions.

The authors wish to thank H. Avakian, A. Afanasev, and M. Schlegel for useful discussions, and the Physics Letters referees for useful suggestions. This work is supported in

part by research grants from the U.S. Department of Energy and the U.S. National Science Foundation. The Southeastern Universities Research Association operates the Thomas Jefferson National Accelerator Facility under the U.S. Department of Energy contract DEAC05-84ER40150.

-
- [1] J. Ashman *et al.*, Phys. Lett. **B 206**, 364 (1988), Nucl. Phys. **B 328**, 1 (1989).
 - [2] P. L. Anthony *et al.*, Phys. Lett. **B 458**, 529 (1999); **B 463**, 339 (1999); **B 493**, 19 (2000).
 - [3] A. Airapetian *et al.*, Phys. Lett. **B 404**, 383 (1997); **B 444**, 531 (1998) Phys. Lett. **B 442**, 484 (1998).
 - [4] J. Adams *et al.*, Phys. Rev. Lett. **92**, 171801 (2004); S. S. Adler *et al.*, Phys. Rev. Lett. **91**, 241803 (2003).
 - [5] X. Ji *et al.*, Phys. Lett. **B 597**, 299 (2004).
 - [6] M. Anselmino, M. Boglione, U. D'Alesio, A. Kotzinian, F. Murgia and A. Prokudin, AIP Conf. Proc. **792**, 981 (2005) [arXiv:hep-ph/0507157]; M. Anselmino, M. Boglione, A. Prokudin and C. Turk, Eur. Phys. J. A **31**, 373 (2007) [arXiv:hep-ph/0606286]; M. Anselmino *et al.*, Phys. Rev. **D71** (2005) 074006; M. Anselmino, M. Boglione, A. Prokudin, and C. Turk, Eur. Phys. J. **A31** (2007) 373.
 - [7] W. Melnitchouk, AIP Conf. Proc. **588**,(2001) 267.
 - [8] T. Navasardyan *et al.*, Phys. Rev. Lett. **98** (2007) 022001.
 - [9] J. T. Dakin *et al.*, Phys. Rev. Lett. **31**, 786 (1973).
 - [10] A.S. Raskin and T.W. Donnelly, Ann. Phys., **191**, 78 (1989).
 - [11] R. N. Cahn, Phys. Lett. **B 78**, 269 (1978); Phys. Rev. D **40** 3107 (1989).
 - [12] J. Levelt and P. J. Mulders, Phys. Rev. **D 49**, 96 (1994).
 - [13] E. L. Berger, T. Gottschalk, and D. W. Sivers Phys. Rev. D **23** (1981) 99.
 - [14] K. Oganessyan *et al.*, Eur. Phys. J. C5 (1998) 681.
 - [15] A. Metz, Phys. Lett. **B549** (2002) 139.
 - [16] A. Bacchetta *et al.* JHEP 0702 (2007), 93.
 - [17] D. Boer and P. J. Mulders, Phys. Rev. **D 57** (1998) 5780; Nucl. Phys. **B 564** (2000) 471; D. Boer and R. D. Tangerman, Nucl. Phys. **B 461** (1996) 197.
 - [18] Vincenzo Barone, Zhun Lu and Bo-Qiang Ma, hep-ph/0512145 (2005).

- [19] A. Afanasev *et al.*, Phys. Rev. D **66** 074004 (2002)..
- [20] N. Makins, Ph. D. Thesis, Massachusetts Institute of Technology (1994), unpublished; R. Ent *et al.*, Phys. Rev. C **64**, 054610 (2001).
- [21] M. Glück, E. Reya, and A. Vogt, Eur. Phys. J. **C5** (1998) 461.
- [22] P. Geiger, Ph.D. Dissertation, Heidelberg University (1998), unpublished.
- [23] R. Jakob, P.J. Mulders, and J. Rodrigues, Nucl. Phys. **A626**, 937 (1997).
- [24] Bino Maiheu, Ph.D Thesis, Universiteit Gent, March 2006 (HERMES DOC 06-061).
- [25] M. Lacombe *et al.*, Phys. Rev. C **21**, 861 (1980).

TABLE I: Differential cross-sections per nucleus for π^\pm production on hydrogen and deuterium versus P_t^2 . The error bars are statistical only. The values of $\cos(\phi)$ and $\cos(2\phi)$ averaged over the experimental acceptance are also indicated (see Fig. 2).

P_t^2 GeV ²	$\langle \cos(\phi) \rangle$	$\langle \cos(2\phi) \rangle$	$\sigma_p^{\pi^+}$ nb/sr/GeV ³	$\sigma_p^{\pi^-}$ nb/sr/GeV ³	$\sigma_d^{\pi^+}$ nb/sr/GeV ³	$\sigma_d^{\pi^-}$ nb/sr/GeV ³
0.008	-0.369	0.031	2.177± 0.075	0.956± 0.021	2.912± 0.038	1.796± 0.030
0.018	-0.511	0.089	2.058± 0.077	0.951± 0.024	2.824± 0.040	1.800± 0.037
0.028	-0.533	0.105	1.885± 0.082	0.885± 0.030	2.688± 0.045	1.690± 0.045
0.038	-0.875	0.580	1.834± 0.089	0.863± 0.035	2.602± 0.051	1.599± 0.052
0.048	-0.892	0.623	1.815± 0.094	0.825± 0.038	2.504± 0.055	1.567± 0.056
0.058	-0.935	0.761	1.808± 0.097	0.726± 0.040	2.393± 0.060	1.491± 0.060
0.068	-0.941	0.780	1.658± 0.100	0.747± 0.047	2.307± 0.063	1.511± 0.067
0.078	-0.946	0.799	1.575± 0.101	0.683± 0.050	2.247± 0.065	1.344± 0.069
0.088	-0.952	0.818	1.507± 0.105	0.702± 0.053	2.099± 0.069	1.403± 0.074
0.098	-0.963	0.858	1.414± 0.109	0.653± 0.055	1.964± 0.071	1.398± 0.077
0.108	-0.963	0.860	1.477± 0.120	0.520± 0.050	1.980± 0.075	1.208± 0.073
0.118	-0.965	0.866	1.391± 0.129	0.584± 0.056	1.878± 0.079	1.196± 0.077
0.128	-0.963	0.857	1.208± 0.133	0.563± 0.060	1.789± 0.085	1.123± 0.080
0.138	-0.972	0.892	1.112± 0.150	0.589± 0.067	1.768± 0.098	1.131± 0.090
0.148	-0.972	0.892	1.146± 0.176	0.476± 0.069	1.671± 0.111	1.142± 0.105
0.158	-0.973	0.897	1.147± 0.203	0.627± 0.093	1.762± 0.133	0.967± 0.115
0.168	-0.975	0.902	0.868± 0.236	0.280± 0.095	1.316± 0.145	0.795± 0.139
0.178	-0.977	0.911	1.027± 0.307	0.324± 0.119	1.810± 0.222	0.906± 0.182
0.188	-0.977	0.911	0.771± 0.366	0.519± 0.171	1.465± 0.280	1.244± 0.303
0.198	-0.977	0.911	0.847± 0.509	0.579± 0.319	1.740± 0.398	0.357± 0.258